Performance analysis of a large-area luminescent solar concentrator module

N. Aste [a], L.C. Tagliabue [a, *], C. Del Pero [a], D. Testa [b], R. Fusco [b]

[a] Architecture, Built Environment and Construction Engineering Department, Politecnico di Milano, Via Bonardi 9, 20133 Milano, Italy
[b] Eni S.p.A, Research Center for Non-Conventional Energies, ENI Donegani Institute, Via Fauser 4, 28100 Novara, Italy

Received 9 September 2013
Accepted 11 November 2014
Available online 2 December 2014

1. Introduction

Solar energy exploitation plays a key role in the sustainable development and energy efficiency of buildings [1]. The European goals to improve renewable energy and to reduce energy consumption and pollution [2] are strongly based on solar technology, which is one of the preferred ways used to construct "nearly zero-energy buildings" [3]. Although the Building Integrated Photovoltaic (BIPV) sector is constantly growing [4], the use of standard modules for building integration involves serious constraints: the most efficient components are opaque and have a standard shape, and, in addition, they need a high availability of direct solar irradiation.

When transparency and a more extensive use of diffuse radiation are required, LSCs components may be a good alternative to traditional PV [5]. However, their durability and technical-economic competitiveness must be ensured [6].

The first experiments on LSC can be found already in the late 1970s [7–9] when the total internal reflection (TIR) effect of specific dyes was discussed to implement solar components with reduced PV surface, in order to minimize the costs of the technology. Furthermore, the crucial issues of self-absorption, constraining size and shape of the components and different dyes and guest materials were studied [10–12]. Commercial dyes are now available and this paper describes a new component which uses a mix of two dyes (i.e. a commercial dye and a custom-produced dye), which improves the energy performance.

This paper describes, in section 2, the operating principles of the LSC analyzed, while in section 3 a characterization of the component in different configurations is carried out (i.e. a free plate and a plate equipped with a frame), based on LSCs specific parameters deduced by technical literature. During the research, the LSC prototype developed was assembled in a LSC module, which underwent an outdoor measurement campaign described and discussed in sections 4 and 5. The electrical performance results of the LSC module, compared with those of the traditional PV technologies, are reported in section 5. Section 6 summarizes the conclusions and the follow-up of the research activities on the LSC.

2. Operating principles of LSCs

This work concerns a specific LSC developed by the ENI Donegani Institute and tested at the Politecnico di Milano. The concept consists essentially in a semitransparent yellow plate with PV cells

* Corresponding author. Tel./fax: +39 02 2399 9469.
E-mail address: chiara.tagliabue@polimi.it (L.C. Tagliabue).

on the edges. Dye molecules are dispersed into a square transparent plastic polymethylmethacrylate (PMMA) sheet and strips of single crystalline solar cells (Sc−Si) are glued to the four edges of the plate. The Sc−Si PV technology used was chosen due to its good efficiency as well as to technical-economic reasons.

Fig. 1 shows the operating scheme of the LSC. Fluorescent molecules act as spectrum converters: they absorb and emit photons with different frequencies. The photons emitted from a molecule of dye spread into the plate and, due to total internal reflection, are concentrated at the edges of the slab, where the photovoltaic cells are located. The silicon-based solar cells absorb and convert visible radiation and part of the infrared radiation [13] as discussed in section 4, according to the external quantum efficiency (EQE) curve plotted in Fig. 5. The features of the LSC panel allow a better exploitation of the cells by means of the spectrum conversion, shifting solar radiation to more favorable wavelengths and, in addition, reducing the self-absorption effect of the dyes.

Furthermore, the possibility to direct and concentrate solar radiation to the edges of the panel by total internal reflection (TIR) allows to minimize the PV surface [14].

The specific concentration of the dyes in the guest material, which is about 100 ppm, makes it possible for a 25% of the whole solar radiation incident on the aperture area (i.e. the front surface) of the LSC plate to be absorbed, while the remaining 75% passes through. Then, part of the absorbed radiation hits the solar cells at the edges, with a subsequent change of the spectrum and of the related energy content.

The solar radiation absorbed by the fluorescent molecules at frequency ν_1 is emitted at a lower frequency ν_2, at which it is subjected to a lower self-absorption by the other fluorescent molecules.

Therefore, the crucial self-absorption problem is minimized and the re-emitted radiation, guided by total internal reflection, is concentrated on the edges of the solar cells.

The LSC panel realized by ENI Donegani Institute uses a 50 × 50 cm PMMA plate, 6 mm thick, doped with two dyes: DTB (4,7-di(2-thienyl)benzo[c]1,2,5-thiadiazole) synthesized by ENI, and DPA (9,10-diphenylanthracene), a commercial dye (Patent Number(s): WO2011048458-A1; WO2011048458-A8).

The curves of absorption and photoluminescent intensity of emission related to the two dyes are shown in Fig. 2. It can be noted that the peaks of absorption of the DTB dye are located at 300 and 450 nm and the emission peak is at about 600 nm. The DPA dye has peaks of absorption around 350 and 400 nm and peaks of emission

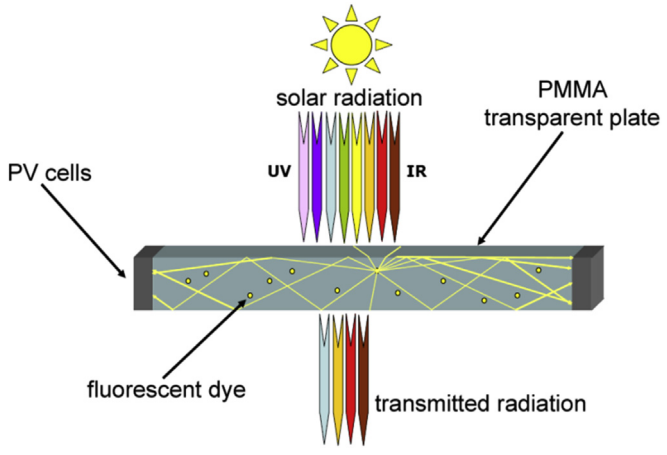

Fig. 1. Diagram of the incident photons and of the photons emitted by a dye molecules inside the LSC (source: ENI Donegani Institute).

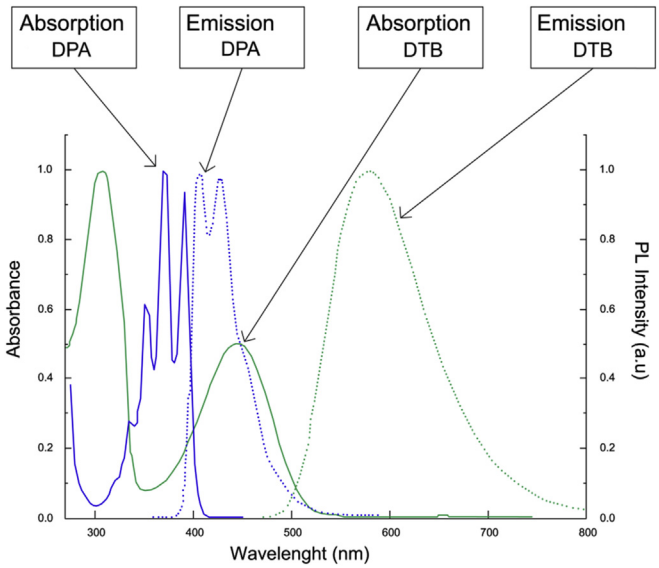

Fig. 2. Absorbance and emission spectra of DTB and DPA in PMMA; experimental measurements carried out at ENI Donegani Institute.

at 420 and 450 nm. Thus the dyes perform a shifting of the wavelength from the ultraviolet to the visible and infrared (IR) light, more favorable to PV devices with respect to the specific PV cells used.

The LSC panel is equipped with 88 monocrystalline PV cells, 22 × 7 mm each, in a combined series-parallel connection, assembled with silicone into the four edges of the plate (Fig. 3). The characteristics of the cells are listed in Table 1.

By assembling six 50 × 50 cm panels in a single metal frame, a 108.4 × 161.8 cm LSC module was realized, as shown in Fig. 4. The total nominal power of the 528 cells installed in the module amounts to 11.77 W_p.

3. LSC panel characterization

Primary experimental evaluations were carried out at ENI Donegani Institute to define the basic characterization of the LSC panel.

In order to calculate the electric gain and the efficiency of the LSC component, it is possible to refer to some specific parameters, as described hereafter.

First, the electric gain (γ_p) of a single cell of the LSC is defined as the ratio between the ideal output power of the cell [15,16] and that of a reference PV cell, according to the following equation [17], where quantities are referred to Standard Test Conditions (STC):

$$\gamma_p = \frac{I_{sc,LSC} V_{oc,LSC}}{I_{sc,REF} V_{oc,REF}} \quad (1)$$

where:

$I_{sc,LSC}$ is the short circuit current of the cell integrated in the LSC plate [A];
$V_{oc,LSC}$ is the open circuit voltage of the cell integrated in the LSC plate [V];
$I_{sc,REF}$ is the short circuit current of the reference PV cell [A];
$V_{oc,REF}$ is the open circuit voltage of the reference PV cell [V].

The reference cell is a PV cell with the same area and characteristics as the ones integrated in the LSC plate, and with the same tilt and azimuth angles of the LSC plate.

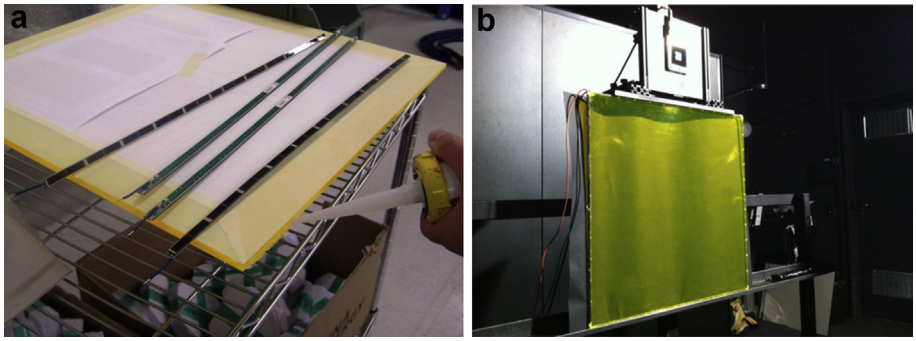

Fig. 3. (a) Assembly of the PMMA panel with the crystalline PV cells and (b) Flash Test of the panel performed at the SUPSI (University of Applied Sciences and Arts of Southern Switzerland) Institute laboratories.

Table 1
Characteristics of the photovoltaic cells.

	Units	
Technology		Sc–Si
Gross area	[cm^2]	1.54
Active area	[cm^2]	1.01
Maximum power P_{mpp}	[mW]	22.3
Maximum power voltage V_{mpp}	[V]	0.5
Maximum power current I_{mpp}	[mA]	44.6
Short circuit current I_{sc}	[mA]	50
Open circuit voltage V_{oc}	[V]	0.63
Temperature coefficient αV_{oc}	[%/°C]	−0.33
Cell efficiency (on active area)	[%]	22

Afterwards, the ratio between the ideal power of the cells attached to the four edges of the LSC panel along the perimeter and the power produced by a PV surface equivalent to the LSC aperture surface is defined as the overall electric gain (Γ_p). The equation describing this parameter can be written as:

$$\Gamma_p = \frac{\gamma_p}{\Gamma} \tag{2}$$

where:

γ_p is the electric gain [−];
Γ is the geometric gain, defined as the ratio of the aperture surface and the edge area of the collector [−]; for square plates it can be calculated as:

Table 2
Main characterization parameters of the LSC panel by the ENI Donegani Institute.

Parameter	Symbol	Unit	Simple LSC	LSC with edge frame
			nEF	EF
Geometric gain	Γ	[−]	20.83	20.42
Electric gain	γ_p	[−]	1.19	0.97
Overall electric gain	Γ_p	[−]	0.06	0.05
Electric efficiency	η_e	[%]	1.26	1.03
Optical efficiency	η_{opt}	[%]	6.4	5.3

$$\Gamma = \frac{L}{4d} \tag{3}$$

where:

L is the length of the LSC plate's side [cm].
d is the thickness of the LSC plate [cm];

The electric efficiency (η_e) of the LSC panel, which depends on the aperture area, type of dye and technology of the PV cells, can thus be defined as:

$$\eta_e = \Gamma_p \eta_{PV} \tag{4}$$

where η_{PV} is the efficiency of the PV cells integrated in the LSC component [%].

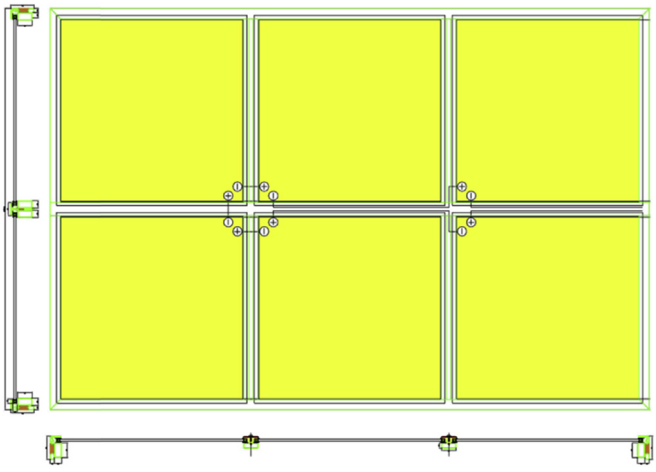

Fig. 4. LSC module made by six LSC panels assembled in the custom-designed metal frame.

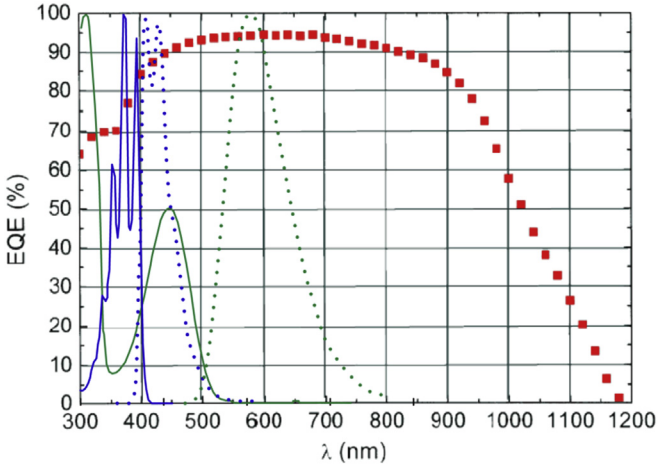

Fig. 5. External quantum efficiency of the Sc–Si cells (square dots) and wavelength of absorption (continuous line) and emission (dot line) of the DTB and DPA dyes.

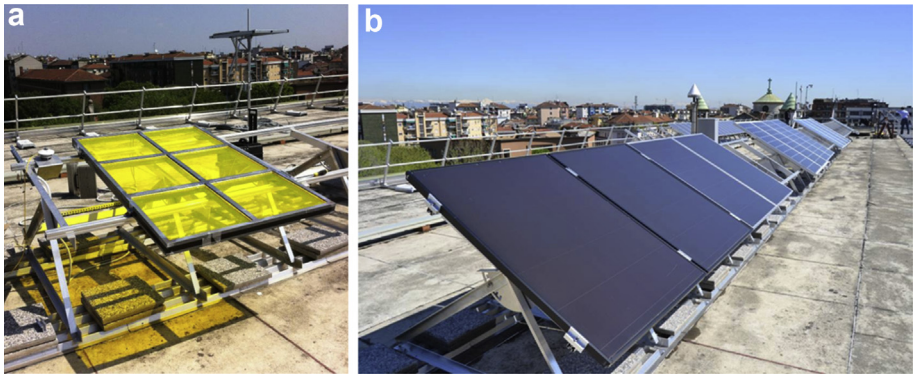

Fig. 6. (a) ENI module and (b) standard photovoltaic modules at the PV Test Facility of the Politecnico di Milano University, Italy.

Table 3
Characteristics of the standard modules compared with the ENI LSC module.

	Units	LSC ENI module	POLI module	MONO module	Tandem module
Technology		Sc–Si	Mc–Si	Sc–Si	μc–Si
Module area	[m^2]	1.75	1.63	1.63	1.421
Cells area	[m^2]	0.053	1.46	1.42	1.45
Maximum power P_{mpp}	[W]	14.08	240.21	250.00	148.80
Maximum power voltage V_{mpp}	[V]	24.29	30.10	30.60	49.20
Maximum power current I_{mpp}	[A]	0.58	7.98	8.20	3.02
Short circuit current I_{sc}	[A]	0.63	8.50	8.61	3.45
Open circuit voltage V_{oc}	[V]	30.16	37.54	37.40	59.80
Temperature coefficient αV_{oc}	[%/°C]	−0.33	−0.42	−0.44	−0.30

Finally, because the real performance of a LSC is correlated to its optical characteristics, it is important to calculate the optical efficiency (η_{opt}). This parameter is affected by a series of factors [18,19] but can be calculated by the following simplified equation [20]:

$$\eta_{opt} = \frac{\dot{P}_{LSC}}{\dot{P}_{REF}} \frac{1}{\Gamma} \tag{5}$$

where:

$\dot{P}_{LSC}$ is the output power density of the solar cell integrated in the LSC [W/m^2];
$\dot{P}_{REF}$ is the output power density of the reference cell [W/m^2];
Γ is the geometric gain, defined in equation (3) [−].

As described in section 4 below, the flow of solar radiation through the LSC plate causes a modification of the spectrum and consequently – due to the spectrum shift – quantum efficiency changes between the LSC integrated cell and the reference PV cell; for this reason, equation (5) represents a simplified method to calculate optical efficiency (η_{opt}).

According to the previously reported definitions, the specific values of various parameters related to two different configurations of the LSC panel analyzed, with an edge frame (EF) and without an edge frame (nEF), were calculated and summarized in Table 2. The data reported are calculated on the values registered during the Flash Tests performed at SUPSI Institute in Standard Test Conditions (STC).

It can be noted that an edge frame of 0.5 mm, realized with opaque adhesive tape to simulate the presence of the frame needed to integrate the panel in a hypothetic building component, causes a

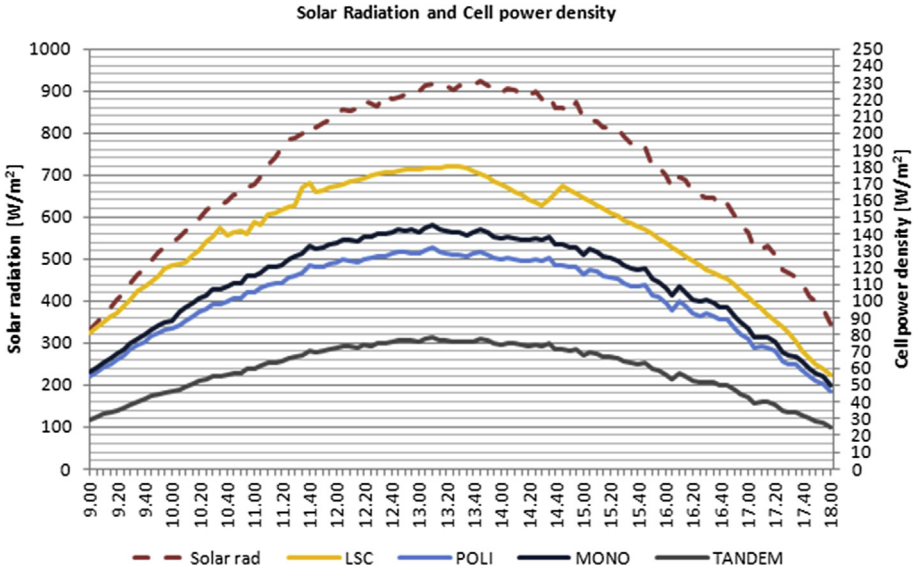

Fig. 7. Sunny day: cell power density of the different modules and solar radiation monitored.

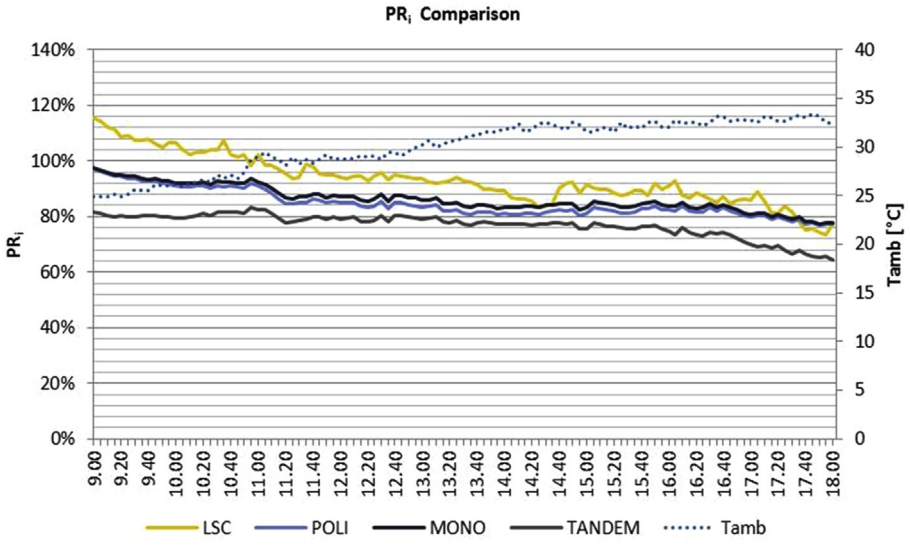

Fig. 8. Sunny day: performance ratio comparison between the different modules and air temperature.

reduction of the aperture area of 2%, with a consequent decrease of the electric and optical efficiency of about 1/6.

In view of the size and the technologies used in the LSC plate realized by ENI Donegani Institute, the electric and optical performances can be considered high [21–25].

4. LSC module testing

Previously defined equations and parameters refer to a single LSC plate; however, the aim of this study is to extend the concept from the plate to a whole component, i.e. a LSC module. In this case it is interesting to evaluate the LSC performances compared to one or more standard PV modules, rather than to a single reference cell.

For this reason a wider analysis is carried out and equation (5) has been calculated for the LSC module under analysis, comparing the results obtained to those of three standard PV modules. In this sense, the equation (5) can be written as follows:

$$\eta_{opt} = \frac{\dot{P}_{LSC} A_{LSC}}{\dot{P}_M A_M} = \frac{P_{LSC}}{P_M} \tag{6}$$

where:

$\dot{P}_{LSC}$ is the maximum output power density of the solar cell integrated in the LSC [W/m^2];
A_{LSC} is the active area of the cells integrated in the LSC module, considering all the LSC slabs constituting the component [m^2];
$\dot{P}_M$ is the maximum output power density of the module used as reference [W/m^2];
A_M is the active area of the module used as reference [m^2];
P_{LSC} is the maximum output power of the LSC module [W];
P_M is the maximum output power of the module used as reference [W].

Equation (6) compares the power of the LSC module to a reference PV module. More in detail, in this study the performances of the LSC module analyzed are compared to PV modules of different technologies (crystalline and thin film silicon), tested in the same climatic conditions. In this way, it is possible to analyze in depth the advantages that can be achieved by the LSC component.

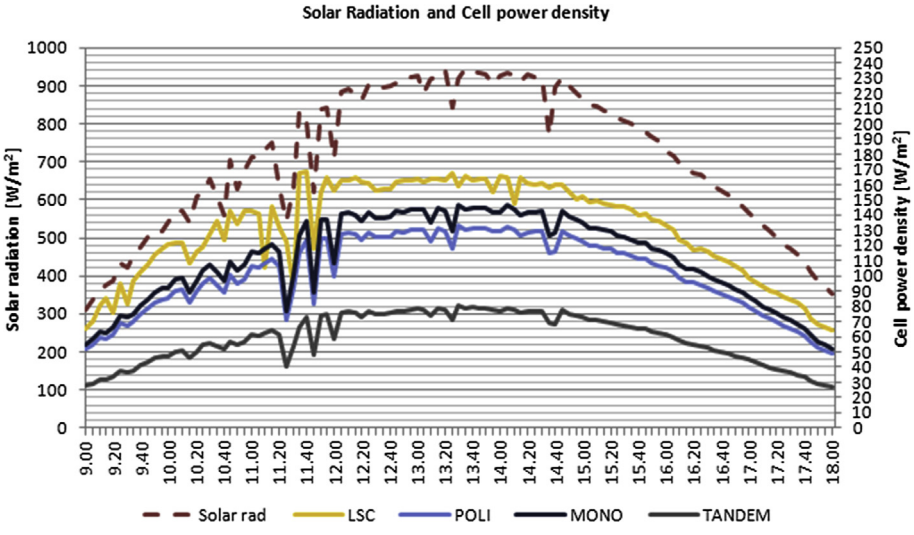

Fig. 9. Partially cloudy day: cell power density of the different modules and solar radiation monitored.

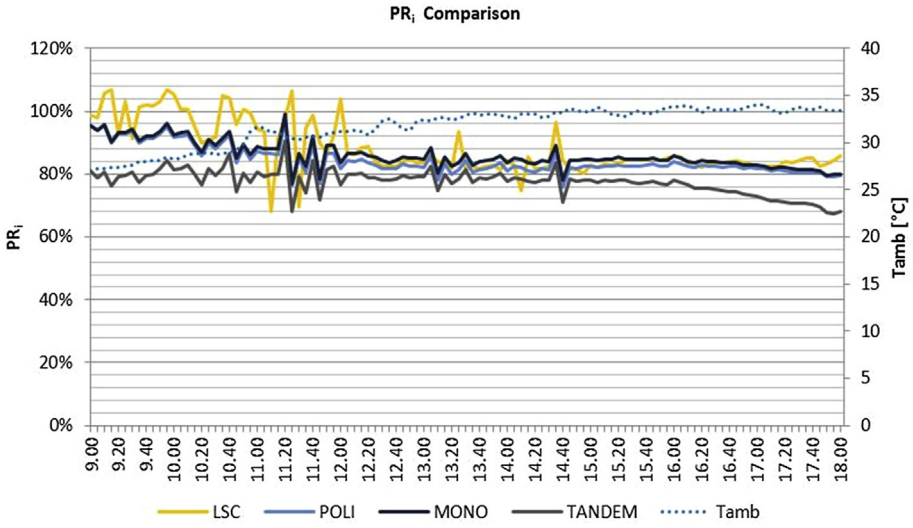

Fig. 10. Partially cloudy day: performance ratio comparison between the different modules and air temperature.

Moreover, equations (5) and (6) describe the optical performance of the LSC device only, focusing on the concentrating factor.

However the operating behavior of the LSC module presents further advantages, thanks to the reduction of the reflective losses and, primarily, allowing a better exploitation of the solar radiation [26]. The dyes, in fact, absorb the solar radiation and re-emit it into a spectrum more favorable to the PV conversion with respect to the specific PV cell used. Fig. 5 shows the shifting between the absorbed and the re-emitted spectrum towards the most effective areas of the quantum efficiency curve of the PV cells.

As it is well known, the quantum efficiency is an important parameter to evaluate the performance and the quality of a solar cell; the two declinations of this parameter are the external quantum efficiency (EQE) and the internal quantum efficiency (IQE) [27]. EQE measures the ratio between collected electrons and incident photons, as a function of the wavelength of the incident monochromatic light. Similarly, IQE is the ratio of collected electrons and absorbed photons as a function of the wavelength. The two parameters are connected by the light absorption capacity or light harvesting efficiency (LHE) of the absorbing material as a function of the wavelength [28].

In Fig. 5 the EQE is plotted as a function of the wavelength of the solar cells used in the LSC module analyzed and it is overlapped to the absorption and emission curves of the two dyes casted in the PMMA (see Fig. 2).

In order to analyze in real operating conditions all the described features of the LSC module investigated, using an all-comprehensive parameter, in this work the PV performance ratio (PR) was considered.

In detail, the PR measures the deviation between the actual performances of a PV system and those theoretically achievable working at Standard Test Conditions (except for solar irradiance) [29] and can be defined both on output electrical power and on produced energy, according to the following formulas:

$$\mathrm{PR_i} = \frac{P_\mathrm{i}}{\frac{G}{G_\mathrm{stc}} \times P} \tag{7}$$

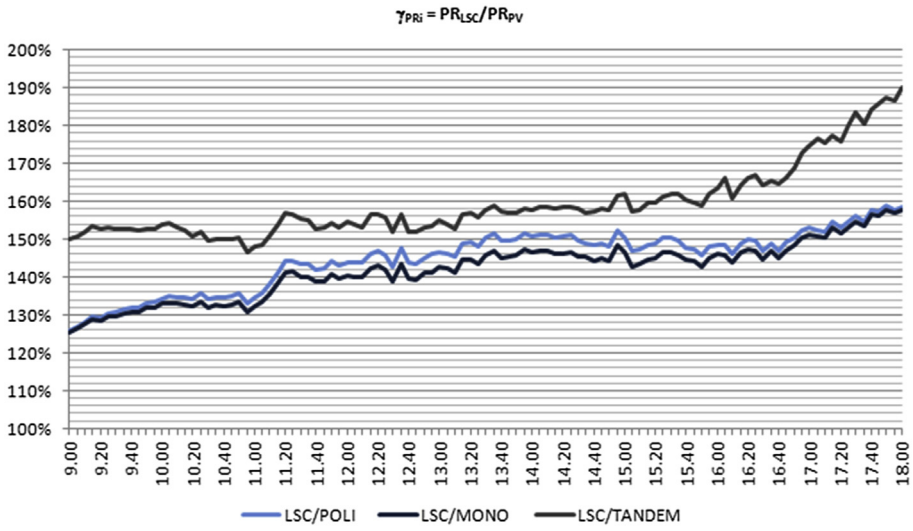

Fig. 11. Sunny day: PR_{LSC}/PR_{PV} daily performance ratio related the LSC ENI module and the standard PV modules.

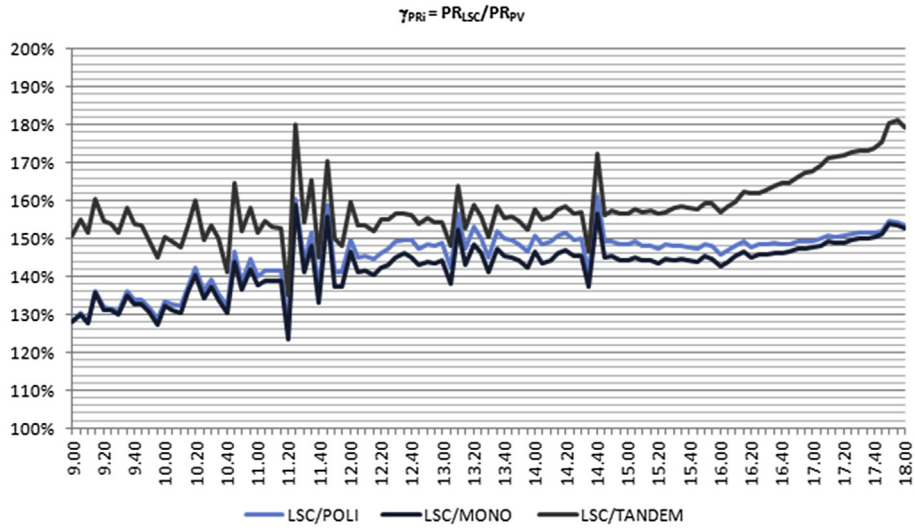

Fig. 12. Partially cloudy day: PR_{LSC}/PR_{PV} daily performance ratio related the LSC ENI module and the standard PV modules.

$$PR_d = \frac{E}{\frac{H}{G_{stc}} \times P} \tag{8}$$

where:

PR_i is the instantaneous performance ratio [−];
P_i is the output power generated in direct current by the module [W];
G is the solar irradiance on the module [W/m^2];
P is the STC power of the module [W];
PR_d is the daily performance ratio [−];
E is the energy generated in direct current during a day [Wh];
H is the daily solar irradiation on the PV module [Wh/m^{2}day].
G_{stc} is the irradiance at STC, equal to 1000 W/m^2.

The calculation of the PR_i and PR_d parameter in outdoor conditions was carried out by field measurements. Moreover, in order to assess the confidence on results, an uncertainty analysis on measurements was performed; in detail, for multiplied or divided independent quantities, the uncertainty on the result can be obtained by calculating and then adding up the fractional uncertainties, according to the specifications of the measuring instruments, which are the following:

- Solar irradiance, acquired by a solarimeter equipped with a photodiode sensor: ±4%;
- Electrical power, acquired by a multifunction testing device with voltage and current sensors: ±1%;
- Module temperature, measured by a PT100 sensor: ±3%;

As a consequence, the final maximum uncertainty on PR could be considered as being equal to ±5%;

In detail, electrical output measurements were conducted on six sample days (3 sunny days and 3 partially cloudy days), in August 2012, and the LSC performance was analyzed in comparison with the reference standard PV modules. The tests were carried out in Milan, Italy, at the PV Test Facility of the Politecnico di Milano University. All monitored modules, including LSCs, were positioned facing south, with a tilt angle of 30°. As introduced before, the comparative analysis described in this paper is based on the operating data collected from three reference standard PV modules (crystalline and thin film) and from the LSC module (Fig. 6).

The technical parameters of the different modules are summa-rized in Table 3.

5. Test results

Figs. 7−10 show the measured and calculated data related to a day with a perfectly clear sky and a clear day with occasional clouds (hereafter defined “partially cloudy”), in order to test the response to variable irradiance. The power density generated by the LSC module, referred to the actual active PV cell surface, is comparable to that generated by the standard modules, although the transparent LSC absorbs only 25% of the solar radiation (about 75% is transmitted).

During sunny days, the PR_i graph shows higher values for the LSC module in a range between 20 and 40%, depending on the technology being compared (higher variations refer to tandem thin film cells). During partially cloudy days, the PR_i values for the LSC module are even higher, up to 30−45% higher than the PV standard modules. It can be noted that PR_i decreases during the day, due to the increase of the operating temperature.

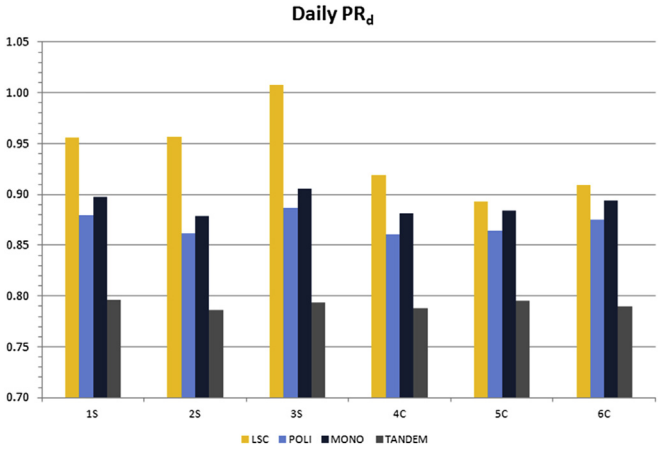

Fig. 13. Daily performance ratio related the ENI module and the standard PV modules. S = sunny days; C = partially cloudy days.

Defining γ_{PRi} as the ratio between the instantaneous performance ratio of the LSC module and that of the photovoltaic modules, the daily trends can be plotted as in Figs. 11 and 12.

It is possible to appreciate that γ_{PRi} is always higher than 100% during both the sunny and the cloudy days, for all the different technologies considered as reference.

Fig. 13 shows the daily performance ratio values (PR_d) on energy produced for the LSC module and the PV reference standard modules.

The PR_d of the ENI LSC module is always higher than the other modules, in particular in clear-sky conditions during the monitoring period.

The relationship between temperature and PR is highlighted in Figs. 8 and 10, which allow to appreciate during the afternoon a decrement of electrical performance, more relevant for the crystalline silicon cells than for the amorphous silicon substrate. The effect of temperature is stronger during sunny days and also the LSC module shows a performance dependent on high temperature; however the cells are not steadily exposed to direct to solar radiation, as in the traditional modules.

The average PR_d value for the crystalline modules is 7% lower than the ENI module value during sunny days and 8% lower during cloudy days. The range of the values goes from 5 to 10% less than the PR_d of the LSC module. The PR_d values of tandem modules are 17–18% lower than the PR_d of the LSC module, registering no relevant differences between sunny and cloudy days.

6. Conclusions

As it was observed, the LSC operating principle allows a wider exploitation of solar cells' quantum efficiency, with a higher conversion rate, which simply means that, in the same conditions, solar cells can perform better in term of performance ratio. In particular, it was observed that the LSC module's performance ratio is generally higher than those of other standard PV modules.

Further work will be performed in order to assess the energy performance of the system in a more extensive monitoring sessions, and to precisely qualify the spectral response of the component.

Finally, the goal of a more detailed testing session that will be carried out in the next months will be the evaluation of the performance of a LSC module installed with different tilt angles, in different climatic conditions and along longer time periods.

It has to be noted that the experiments conducted on the smallest samples at variable exposition and solar irradiation on both surfaces showed higher sensitivity to diffuse radiation [30,31]. Further researches on the LSC response to spatial disposition and solar radiation spectral composition will have to be carried out in the future.

Acknowledgment

The authors would like to mention and acknowledge the SUPSI (University of Applied Sciences and Arts of Southern Switzerland) Institute laboratories for the valuable cooperation in the performance evaluation phase of the prototype.

References

[1] Aste N, Adhikari RS, Del Pero C. Photovoltaic technology for renewable electricity production: towards net zero energy buildings. In: International Conference on Clean Electrical Power (ICCEP); 2011. p. 446–50.

[2] Directive 2009/28/EC of the European Parliament and of the Council of 23 April 2009 on the promotion of the use of energy from renewable sources and amending and subsequently repealing Directives 2001/77/EC and 2003/30/EC. Off J Eur Union 5.6.2009.

[3] Directive 2010/31/EU of the European Parliament and of the Council of 19 May 2010 on the energy performance of buildings (recast). Off J Eur Union 18.6.2010.

[4] Pagliaro M, Ciriminna R, Palmisano G. BIPV: merging the photovoltaic with the construction industry. Prog Photovolt – Res Appl 2010;18:61–72.

[5] Wiegman JWE, van der Kolk E. Building integrated thin film luminescent solar concentrators: detailed efficiency characterization and light transport modeling. Sol Energy Mater Sol Cells 2012;103:41–7.

[6] Debije MG, Verbunt PPC. Thirty years of luminescent solar concentrator research: solar energy for the built environment. Adv Energy Mater 2012;2:12–35.

[7] Weber WH, Lambe J. Luminescent greenhouse collector for solar radiation. Appl Opt 1976;15:2299.

[8] Goetzberger A, Greubel W. Solar energy conversion with fluorescent collectors. Appl Phys 1977;14:123.

[9] Goetzberh A. Fluorescent solar energy collectors: operating conditions with diffused light. Appl Phys 1978;16:399.

[10] Swartz BA, Cole T, Zewail AH. Photon trapping and energy transfer in multiple-dye plastic matrices: an efficient solar energy concentrator. Opt Lett 1977;1:73–5.

[11] Levitt JA, Weber WH. Materials for luminescent greenhouse solar collectors. Appl Opt 1977;16(10):2689.

[12] Reisfeld R, Neuman S. Planar solar energy converter and concentrator based on uranyl-doped glass. Nature 1978;274:144–5.

[13] Scudo PF, Abbondanza L, Fusco R, Caccianotti L. Spectral converters and luminescent solar concentrators. Sol Energy Mater Sol Cells 2010;94:1241–6.

[14] Van Sark WGJHM. Luminescent solar concentrators – a low cost photovoltaics alternative. Renew Energy January 2013;49:207–10.

[15] Okada T, Kaneko M. Molecular catalysts for energy conversion. Springer-Verlag Berlin Heidelberg; 2009.

[16] Kakani SL. Electronics theory and applications. New Dehli: New Age International Pvt Ltd Publishers; 2004.

[17] Sidrach de Cardona M, Carrascosa M, Meseguer F, Cusso F, Jaque F. Outdoor evaluation of luminescent solar concentrator prototypes. Appl Opt 1985;24(13):2028–32.

[18] Gramde M, Moss G, Milward S, Saich M. The application of thin-film wavelength-shifting coatings of perspex to solar-energy collection. J Phys D – Appl Phys 1983;16:2525–35.

[19] Sansregret J, Drake JM, Thomas WRL, Lesiecki ML. Light transport in planar luminescent solar concentrators—the role of DCM self-absorption. Appl Opt 1983;22:573–7.

[20] Salem AI, Mansour AF, El-Sayed NM, Bassyouni AH. Outdoor testing and solar simulation for oxazine 750 laser dye luminescent solar concentrator. Renew Energy 2000;20:95–107.

[21] Friedman PS. Calculation of luminescent solar concentrator efficiencies, LSC contract report. Owens-Illinois; 1980. SERI Contract XS-9-8216-1.

[22] Batchelder JS, Zewail AH, Cole T. Luminescent solar concentrators. 2: experimental and theoretical analysis of their possible efficiencies. Appl Opt 1981;20:3733.

[23] Heidler K, Goetzberger A. Fluorescent planar concentrator (FPC): Monte-Carlo computer model. Limit efficiency and latest experimental results. In: Proceedings, Fourth E. C. Photovoltaic Solar Energy Conference, Stresa, Italy; 1982.

[24] Slooff LH, Bende EE, Burgers AR, Budel T, Pravettoni M, Kenny RP, et al. A luminescent solar concentrator with 7.1% power conversion efficiency. Phys Status Solidi (RRL) 2008;2(6):257–9.

[25] Van Sark WGJHM, Barnham KWJ, Slooff LH, Chatten AJ, Büchtemann A, Meyer A, et al. Luminescent solar concentrators – a review of recent results. Opt Express 2008;16(26):21773–92.

[26] Earp AA, Smith GB, Swift PD, Franklin J. Maximising the light output of a luminescent solar concentrator. Sol Energy 2004;76:655–67.

[27] Wilson LR, Richards BS. Measurement method for photoluminescent quantum yields of fluorescent organic dyes in polymethyl methacrylate for luminescent solar concentrators. Appl Opt 2009;48:212–20.

[28] Dienel T, Bauer C, Dolamic I, Bruhwiler D. Spectral-based analysis of thin film luminescent solar concentrators. Sol Energy 2010;84:1366–9.

[29] Aste N, Del Pero C. Technical and economic performance analysis of large-scale ground-mounted PV plants in Italian context. Prog Photovolt Res Appl 2010;18:371–84.

[30] Pravettoni M, Virtuani A, Kenny RP, Farrel DJ, Chatten AJ, Barnham KWJ. Outdoor characterisation of high efficiency luminescent solar concentrators. MRS Proc 2009:1168.

[31] Pravettoni M, Pravettoni F, Virtuani A, Kenny RP, Chatten AJ, Barnham KWJ. Outdoor characterization of luminescent solar concentrators and their possible architectural integration on a historically relevant site in Milan (Italy). In: Photovoltaic Specialists Conference (PVSC), 2009 34th IEEE000192; 7–12 June 2009. p. 000187.